NANO LETTERS

pubs.acs.org/NanoLett

Electrically Facilitated Translocations of Proteins through Silicon Nitride Nanopores: Conjoint and Competitive Action of Diffusion, Electrophoresis, and Electroosmosis

Matthias Firnkes,[†] Daniel Pedone,[†] Jelena Knezevic,[†] Markus Döblinger,[‡] and Ulrich Rant*[,†]

[†]Walter Schottky Institute, Technische Universitaet Munich, Am Coulombwall 3, 85748 Garching, Germany, and [‡]Chemistry Department, Ludwig Maximilians Universitaet, Butenandtstrasse 11, 81377 Munich, Germany

ABSTRACT Solid-state nanopores bear great potential to be used to probe single proteins; however, the passage of proteins through nanopores was found to be complex, and unexpected translocation behavior with respect to the passage direction, rate, and duration was observed. Here we study the translocation of a model protein (avidin) through silicon nitride nanopores focusing on the electrokinetic effects that facilitate protein transport across the pore. The nanopore zeta potential ζ_{pore} and the protein zeta potential $\zeta_{protein}$ are measured independently as a function of solution pH. Our results reveal that electroosmotic transport may enhance or dominate and reverse electrophoretic transport in nanopores. The translocation behavior is rationalized by accounting for the charging states of the protein and the pore, respectively; the resulting translocation direction can be predicted according to the difference in zeta potentials, $\zeta_{protein} - \zeta_{pore}$. When electrophoresis and electroosmosis cancel each other out, diffusion becomes an effective (and bias-independent) mechanism which facilitates protein transport across the pore at a significant rate.

KEYWORDS Nanopore, proteins, surface charge, electroosmosis, electrophoresis

Nanopores have evolved into powerful devices to study and examine single molecules.[1−3] Information about the molecule under investigation (nucleic acids, proteins, small molecules, etc.) is inferred from fluctuations in the trans-pore ionic current which arise when the molecule transiently resides inside the pore while being pulled through the pore by externally applied electric forces. In the past, this scheme has worked particularly well for DNA; here, it is generally accepted that the force which drives the negatively charged DNA through the pore toward the positively biased anode is of electrophoretic (EP) nature.[4−6] In the Helmholtz−Smoluchowski limit for high ionic strength (Debye screening length ≪ particle diameter) the electrophoretic velocity v_{EP} of a particle in an external electric field E is related to the particle charge via its zeta potential $\zeta_{particle}$ (i.e., the electric potential at the particle's slip plane) by

$$v_{EP} = \frac{\varepsilon}{\eta}\zeta_{particle}E \qquad (1)$$

($\varepsilon = \varepsilon_0\varepsilon_r$, η is the solution viscosity).[7] Recently, proteins and peptides have become an important focus of nanopore investigations.[8−12] Aside from their biological counterparts, solid-state nanopores are particularly appealing for this purpose, not only because of their mechanical robustness, but especially because of the possibility to engineer the pore with respect to its size, structure, and surface properties.[13−16] Understanding the translocation behavior of proteins is, however, a challenging task since proteins are only several nanometers in size and feature diverse chemical compositions and complex structures. Moreover, in contrast to strongly and homogeneously charged biopolymers like DNA, the charge of a protein may be distributed irregularly on its surface and can be positive, vanish, or be negative depending on the solution pH. Thus, a fundamental question in the context of electrically assisted translocation is: what drives proteins into, through, and out of nanopores?

In fact, "anomalous" translocation behavior through pores in silicon nitride membranes has been reported[10] and was also observed by ourselves: positively (negatively) charged proteins crossed the pore toward the positively (negatively) charged electrode. Clearly, the direction of these translocations cannot be understood by electrophoresis, so we assumed that electroosmotic (EO) effects might be involved. EO flow occurs in micro- and nanochannels with charged sidewalls:[7,17] an electric field applied along the channel sets the electrical double layer (DL), which screens the surface charge, in motion. The DL drags the fluid along and as a result a net flow is created which, if the Debye length is much smaller than the channel width, features a pluglike velocity profile with the electroosmotic velocity v_{EO} given by

* Corresponding author: telephone, +49 89 289 12778; e-mail, rant@wsi.tum.de.
Received for review: 03/11/2010
Published on Web: 05/03/2010

DOI: 10.1021/nl100861c | *Nano Lett.* **2010,** *10,* 2162–2167

$$v_{EO} = -\frac{\varepsilon}{\eta}\zeta_{wall}E \qquad (2)$$

EO effects have been observed in micrometer to millimeter long nanochannels[18,19] and in carbon nanotube membranes[20] and have been discussed in the context of ion current rectification/ion selectivity in nanopores.[21] Yusko et al. observed EO in long (275 nm), but not in short (10 nm), cylindrical SiN nanopores of 30 nm diameter.[22] Wong and Muthukumar theoretically studied EO in nanopores to rationalize enhanced DNA capture rates.[23] Changes in the binding of cyclodextrin to a biological pore, α-hemolysin, were attributed to EO flow.[24] We address the question whether EO flow of sufficient magnitude can develop in extremely short (order of 10 nm) solid-state channels, which would actually facilitate protein transport.

Here we study the translocation behavior of a model protein (avidin) through a 20 nm wide and 30 nm long nanopore in a SiN membrane. We investigate the influence of the protein zeta potential ($\zeta_{protein}$) and the pore wall potential (ζ_{pore}) on the translocation direction and the translocation rate. At first we separately characterize $\zeta_{protein}$ and ζ_{pore} in solution as a function of varying pH. Then, we present measurements of the translocation behavior of avidin through the pore at varying pH values and discuss different cases where the protein and the pore are likewise positively or negatively charged and where the protein and the pore are oppositely charged. We argue that the protein translocation direction and rate are governed by a combined action of EP and EO forces and diffusion.

Protein Zeta Potential, $\zeta_{protein}$. We measured the electrophoretic velocity of avidin in ac electric fields in solution by phase analysis light scattering (PALS laser Doppler electrophoresis) using a Zetasizer Nano instrument (Malvern Ltd., U.K.). At first, $\zeta_{protein}$ was determined in low ionic strength solutions (10 mM Tris, adjusted with HCl or NaOH to the desired pH) from the mobility μ in the Hückel−Onsager limit $\mu = 2\varepsilon\zeta_{protein}/3\eta$ ($\eta = 10^{-3}$ Pa s, $\varepsilon = \varepsilon_0\varepsilon_r$, $\varepsilon_r = 80$); for higher ionic strengths, the equation was corrected with the Henry function.[25] Figure 1 shows $\zeta_{protein}$ of avidin for different pH values, along with the hydrodynamic diameter (D_h) as determined by dynamic light scattering (DLS). $\zeta_{protein}$ is positive for pH ≤ 8, then drops rapidly, crosses 0 mV between pH 9 and 9.5, and becomes negative for pH > 9.5. Hence, the pI value is 9.3 ± 0.2. D_h stays approximately constant within 6 ± 1 nm over the investigated pH range, indicating that the protein stays intact, i.e., does not unfold, under these conditions, which is in agreement with other reports.[26]

Because electrical experiments with nanopores are usually performed with solutions of high conductance (high salinity), we studied the salt concentration dependence of $\zeta_{protein}$. Figure 1c shows that $\zeta_{protein}$ quickly decreases with increasing KCl concentration (in accordance with observations for other biomaterials and minerals[27−30]) and saturates at roughly 50% of the low ionic strength value when [KCl] ≥ 50 mM. A determination of the electrophoretic mobility at higher salt concentrations was impeded by experimental limitations (high voltages, high currents), but the absence of protein aggregation as evidenced by DLS (see SI Figure 1 in Supporting Information) even at KCl concentrations up to 400 mM, strongly suggests that the proteins retain their charged nature at high ionic strength. In comparison, protein solutions where the pH value was adjusted close to pI were unstable and protein aggregation was observed. The pH dependence of $\zeta_{protein}$ representative for the "high ionic strength" ([KCl] = 50 mM) case is shown as open symbols in Figure 1a.

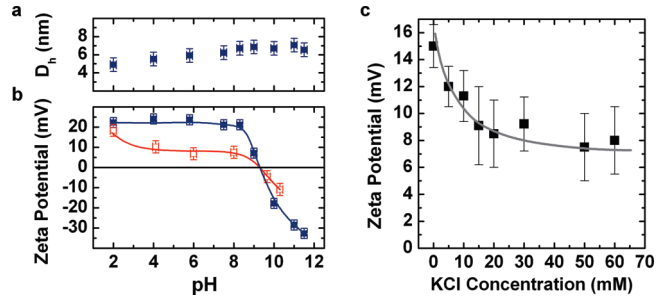

FIGURE 1. Hydrodynamic diameter D_h and zeta potential $\zeta_{protein}$ of avidin as a function of solution pH (a, b). Solid and open symbols denote measurements in 10 mM buffer (see Supporting Information) without and with 50 mM KCl, respectively. (c) Dependence of the zeta potential on solution salinity. Solid lines are guides to the eye. Data points are mean values of three to six measurements.

Nanopore Zeta Potential, ζ_{pore}. Nanopores were fabricated in free-standing 30 nm thick SiN membranes by direct milling with a 300 keV electron beam in a transmission electron microscope;[31] details can be found in the Supporting Information. The zeta potential of the inner pore walls in the SiN membrane was determined by streaming potential measurements.[32,33] For that purpose, the nanopore chip was installed in a home-built pressure cell where the chip is sandwiched between two fluidic compartments to which a differential static pressure of up to 3 bar could be applied. The streaming potential was determined by adjusting the potential applied to Ag/AgCl electrodes, immersed on either side of the pore, so that the measured ionic current generated by the pressure driven flow through the pore vanished. The inset of Figure 2b depicts streaming potential values measured for increasing pressure. Readings were sampled for 2 s in intervals of 10 s for each pressure step and found to be stable; hysteresis effects for decreasing pressure steps were not observed (see SI Figure 3 in Supporting Information). Under the assumption of a cylindrical pore, the analysis of the streaming potential does not require the knowledge of the exact pore geometry (as does the analysis of the streaming current), but relies on the conductivity σ_{pore} inside the pore lumen only. Given that the electrical double layer is very thin (Debye length = 0.5 nm at 400 mM KCl) compared to the dimensions of the pore (~20 nm diameter),

DOI: 10.1021/nl100861c | Nano Lett. 2010, 10, 2162--2167

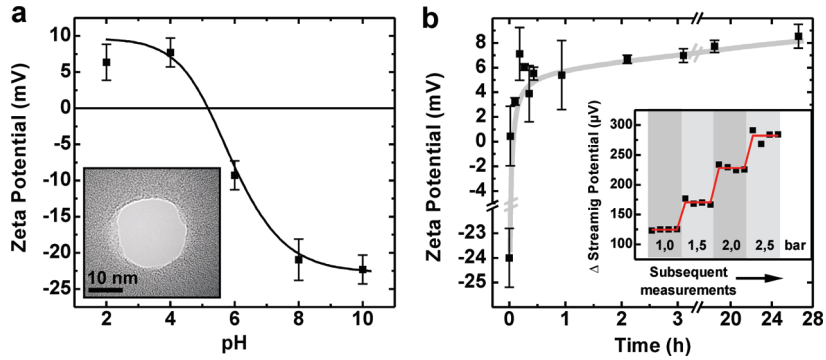

FIGURE 2. Nanopore zeta potential. (a) Zeta potential of a representative Si_3N_4 pore as a function of solution pH 2−10 in 400 mM KCl. Error bars reflect device-to-device variations from three nanopores. Inset: transmission electron micrograph of the used pore. (b) Time evolution of the zeta potential in 400 mM KCl after changing the pH from 10 ($t = 0$) to 4 ($t > 0$). Error bars reflect zeta potential variations of four pressure steps in one measurement. Solid lines are guides to the eye. Inset: Representative streaming potential measurement at varying pressure at pH 4 in 400 mM KCl solution. The red line depicts mean values.

σ_{pore} was approximated by the bulk solution conductivity, i.e., $\sigma_{bulk} = 4.7-5.1$ S/m (depending on pH, measured with a conductometer). ζ_{pore} is obtained by linear regression from a plot of the streaming potential ΔU versus the applied pressure ΔP (see SI Figure 3 in Supporting Information) using the relation[32]

$$\Delta U = \frac{\varepsilon \zeta_{pore}}{\eta \sigma_{pore}} \Delta P \qquad (3)$$

Streaming potential measurements were conducted in solutions of varying pH (2−10) and the obtained zeta potential is presented in Figure 2a. ζ_{pore} is slightly positive for acidic pH values ≤4, crosses 0 mV at pH ∼ 5, becomes increasingly negative at higher pH, and saturates at roughly −25 mV.

The observed trend of ζ_{pore} reflects the chemistry of the silicon nitride surface which tends to hydrate into a surface containing silanol (SiOH) and primary amine ($SiNH_2$) sites.[34] Silanol sites are amphoteric and may become negatively or positively charged ($SiO^-/SiOH_2^+$) while primary amines can become positively charged (NH_3^+). Harame's two-site model[34] predicts that the point of zero charge (pH_{pzc}) adjusts according to the ratio of silanol and amine groups on the surface, which have pK_a values of 2 and roughly 10, respectively. For our devices we estimate from $pH_{pzc} \approx 5$ that one-third of the reactive sites are amines, while two-thirds are silanol groups. It is known that the curve progression depends on the preparation process of the Si_3N_4 surface;[34,35] we observed device-to-device variations of ± 2 mV. Despite the extremely small dimensions of the nanopore, the dependence of the obtained zeta potential on the pH value shows reasonable agreement with the literature, where pH_{pzc} values between 3 and 6 are reported for planar surfaces and long channels.[34,36,37] The fact that our ζ_{pore} values are somewhat smaller in magnitude than other literature reports can be attributed to the high salinity used here. $|\zeta_{pore}|$ increases for lower salt concentration (see SI Figure 4 in Supporting Information), an effect which is expected from theory[30] and is similar to $\zeta_{protein}$.

Figure 2b shows the equilibration of ζ_{pore} after the solution pH was changed from 10 to 4. ζ_{pore} changes rapidly from −24 to +5 mV within half an hour; subsequently, a small and slow increase to +8 mV is observed over 27 h. A similar behavior was described by Bousse et al. for planar Si_3N_4 surfaces.[38] Because the transport properties of Si_3N_4 pores may depend critically on the equilibration time after wetting the chip with fresh buffer solution, we employed a waiting time of at least 12 h during this work.

Protein Translocation at Different pH Values. Figure 3 shows avidin translocation experiments at varying solution pH (results for another protein with a different pI, streptavidin, are described in the Supporting Information). Avidin was added to a solution chamber on one side of the membrane (cis side), which was electrically grounded. Positive or negative potentials (±150 mV) were then applied to the other, trans side of the membrane and the trans-pore ion current was monitored over time. Spikes (pulses) in the current traces are attributed to proteins which pass through the pore lumen, thereby transiently blocking the current flow to some degree. For pH 2, pH 6, and pH 8, the situation appears as intuitively expected: positively charged avidin molecules pass the pore only when the trans side is negatively charged. While this behavior could—like in the case of DNA translocation experiments—be interpreted as electrophoretic transport, the situation is in fact more complex. At pH 10, we clearly observe translocations only when the trans side is negatively biased; however, zeta potential measurements evidently show that at pH 10 avidin is negatively charged (cf. Figure 1b). Contrary to electrophoretic transport, the negatively charged proteins move through the pore toward the negatively charged electrode. Another most remarkable behavior is observed at pH 4: irrespective of the applied bias potentials, avidin translocates the pore as if electrokinetic transport was absent.

DOI: 10.1021/nl100861c | *Nano Lett.* **2010,** *10,* 2162--2167

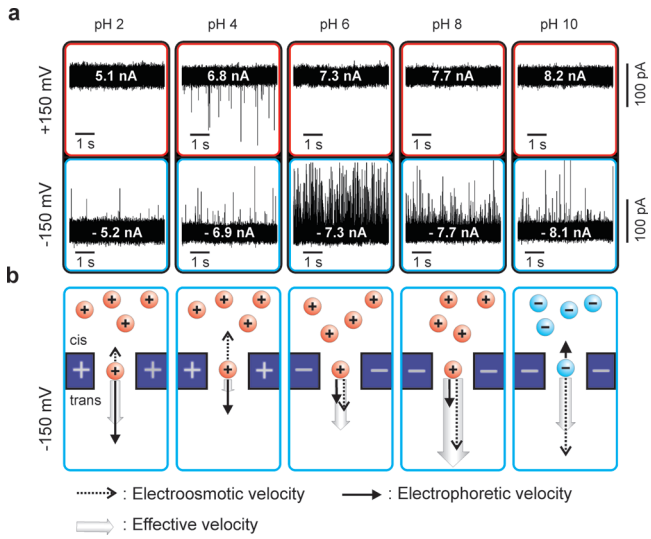

FIGURE 3. (a) Current traces for positive (upper panel) and negative (lower panel) applied bias for varying pH values. Baseline offsets have been adjusted for better comparison, white lettering on top of the traces indicates open-pore currents. A slight increase in the open-pore current was observed over the measurement period (5 days) for the pore used for pH 4−10. A different pore was used for pH 2. (b) Schematic illustrations of protein and pore charges. Arrows represent electroosmotic and electrophoretic velocities, the arrow length is scaled by the respective zeta potentials (cf. Table 1).

To explain these phenomena, we propose that the translocation behavior is governed by a conjoint action of electrophoresis, electroosmosis, and diffusion. Combining the equations for electrophoretic and electroosmotic transport yields an effective velocity v_{eff} of the protein inside the pore

$$v_{\mathrm{eff}} = \frac{\varepsilon E}{\eta}(\zeta_{\mathrm{protein}} - \zeta_{\mathrm{pore}}) \qquad (4)$$

Depending on the signs and relative magnitudes of ζ_{protein} and ζ_{pore}, respectively, electroosmosis may enhance or counteract electrophoresis.

Table 1 summarizes the measured ζ values and permits the experimental observations to be rationalized: For pH 6 and pH 8, EO and EP are unidirectional (parallel) and therefore enhance each other. For pH 2, pH 4, and pH 10, EO flow is directly opposed to the EP movement (antiparallel); yet, the different magnitudes of ζ_{protein} and ζ_{pore} for these pH values give rise to different situations. For pH 2, EO flow weakens the EP movement, but EP still dominates. For pH 10, EO clearly dominates over EP ($|\zeta_{\mathrm{pore}}| \gg |\zeta_{\mathrm{protein}}|$) and the resulting translocation direction is electroosmotic (anti-EP). Translocation events are only observed when the direction of the effective protein velocity in the pore is cis → trans, which (in the case of the SiN/avidin system at hand) occurs for all the pH values mentioned above when the trans side is biased negatively.

In the case of the intermediate pH value 4, the protein and pore zeta potentials are similar, $\zeta_{\mathrm{pore}} \approx \zeta_{\mathrm{protein}}$. Consequently, it is expected that EO flow counterbalances EP flow, the effective velocity of the protein in the pore should vanish ($v_{\mathrm{eff}} \approx 0$), and electrically assisted transport of proteins across the pore does not occur. Remarkably though, we do observe translocation events, which notably do not depend on the direction of the applied bias. We attribute these events to diffusion of proteins through the pore, which is driven by the concentration gradient between the cis and the trans chamber.

Comparing the event rates measured at different pH values (cf. Table 1) we find that the highest event rates are observed at pH values for which EP and EO flow add up (pH 6 and pH 8). Then again we note that for these pH values—in contrast to pH 2, pH 4, and pH 10—the electrical interactions between the pore walls and the protein are *attractive*, i.e., ζ_{pore} and ζ_{protein} feature opposite signs. We can only speculate whether this attraction might contribute to the observed high event rates, for instance by providing a "feeding" mechanism facilitating the collection of proteins from the volume close to the pore mouth, or by slowing the protein inside the pore. The latter effect would result in longer sojourn times, which in turn would enhance the detected event rate, as elucidated below.

Figure 4 shows event distribution plots which correlate the pulse width and pulse height. Two data sets are depicted which represent translocations that are driven by a combined action of EP and EO (pH 8) and translocations that are solely driven by EO flow (against EP, pH 10). Despite the different electrokinetic origin of the translocations, the event distributions are similar. In contrast to other reports from literature,[11,12] we cannot identify several distinct clusters, but find a single pseudocluster point instead. This pseudocluster arises from short current pulses which are

TABLE 1. Pore and Protein Zeta Potentials and Translocation Event Rates for Varying pH

		pH 2[c]	pH 4	pH 6	pH 8	pH 10
zeta potentials (at high ionic strength)						
ζ_{protein} (mV)[a]		18 ± 3	10 ± 3	7 ± 3	8 ± 3	−5 ± 3
ζ_{pore} (mV)[b]		4 ± 4	8 ± 2	−9 ± 2	−21 ± 2	−22 ± 2
$\Delta\zeta$ (mV)		~14	~2	~16	~29	~17
pore−protein interaction		rep.	rep.	attr.	attr.	rep.
event rate (s^{-1})	trans = neg.	2	6	90	40	15
	trans = pos.	0	5	0	0	0

[a] Measured in 50 mM KCl solution. [b] Measured in 400 mM KCl solution. [c] ζ_{pore} and event rates measured with a different SiN pore.

DOI: 10.1021/nl100861c | *Nano Lett.* **2010,** *10,* 2162--2167

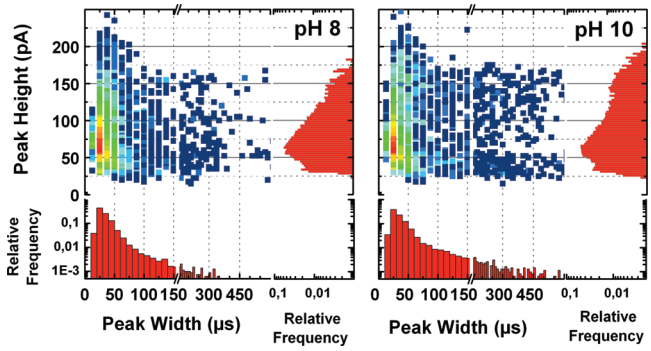

FIGURE 4. Scatter plots of peak height vs peak width of avidin translocation experiments at pH 8 (7900 events) and 10 (6200 events).

attenuated by the employed electronic filters (10 kHz four pole Bessel). From a previous characterization of the time resolution of our setup,[39] we can estimate for the present measurements that current pulses with durations <20 μs will be attenuated to an extent that they cannot be identified by the pulse analysis routine anymore. However, it is likely that most of the proteins cross the pore very rapidly: assuming electrically driven transport with a net $\Delta\zeta$ of ~10 mV and an applied voltage of 0.1 V, v_{eff} becomes >20 nm/μs in the pore, i.e., proteins pass the pore on a time scale of microseconds. On the other hand, the characteristic diffusion time of a protein across a nanopore is of the order of 10 μs (the diffusion coefficient of avidin determined by DLS is 64 $\mu m^2 s^{-1}$). Hence it must be expected that translocations without protein−pore interactions occur on an extremely short time scale and that only a fraction of the actually occurring events are recorded with adequate fidelity.

The results clearly show that EO effects have a major influence on the translocation of moderately charged nanoobjects through nanoscale orifices. For small globular objects like proteins (as opposed to long DNA molecules which normally do not fit through the pore in a coiled state), diffusion in a concentration gradient can also be an efficient mechanism to facilitate directed translocation, in particular when electrokinetic effects cancel each other out.

The electrically assisted translocation direction and rate of proteins through nanopores is governed by EP *and* EO forces. Acting in concert, EO can enhance EP transport, but depending on the zeta potential difference, EO flow may counteract EP and consequently suppress or even reverse EP transport. As a consequence for future nanopore experiments we conclude that the surface charge on the inner pore walls must be carefully controlled when conducting experiments with proteins and that the charging state must be accounted for in the interpretation of protein translocation events.

Acknowledgment. We are very thankful to Gerhard Abstreiter and Thomas Bein for his support. Financial support is gratefully acknowledged from the TUM Institute for Advanced Studies (IAS), the BMBF (Grant 0312031A), and the DFG via SFB 863. We are also thankful for support through the Nanosystems Initiative Munich (NIM) and the TUM International Graduate School of Science and Engineering (IGSSE).

Supporting Information Available. Details of the materials and methods. This material is available free of charge via the Internet at http://pubs.acs.org.

REFERENCES AND NOTES

(1) Howorka, S.; Siwy, Z. *Chem. Soc. Rev.* **2009**, *38* (8), 2360–2384.
(2) Branton, D.; Deamer, D. W.; Marziali, A.; Bayley, H.; Benner, S. A.; Butler, T.; Di Ventra, M.; Garaj, S.; Hibbs, A.; Huang, X.; Jovanovich, S. B.; Krstic, P. S.; Lindsay, S.; Ling, X. S.; Mastrangelo, C. H.; Meller, A.; Oliver, J. S.; Pershin, Y. V.; Ramsey, J. M.; Riehn, R.; Soni, G. V.; Tabard-Cossa, V.; Wanunu, M.; Wiggin, M.; Schloss, J. A. *Nat. Biotechnol.* **2008**, *26* (10), 1146–1153.
(3) Rhee, M.; Burns, M. *Trends Biotechnol.* **2007**, *25* (4), 174–181.
(4) Chen, P.; Gu, J.; Brandin, E.; Kim, Y. R.; Wang, Q.; Branton, D. *Nano Lett.* **2004**, *4* (11), 2293–2298.
(5) Keyser, U. F.; Dorp, S. v.; Lemay, S. G. *Chem. Soc. Rev.* **2010**, *39*, 939–947.
(6) van Dorp, S.; Keyser, U. F.; Dekker, N. H.; Dekker, C.; Lemay, S. G. *Nat. Phys.* **2009**, *5* (5), 347–351.
(7) Schoch, R. B.; Han, J.; Renaud, P. *Rev. Mod. Phys.* **2008**, *80* (3), 839–883.
(8) Movileanu, L. *Trends Biotechnol.* **2009**, *27*, (6).
(9) Sexton, L. T.; Horne, L. P.; Sherrill, S. A.; Bishop, G. W.; Baker, L. A.; Martin, C. R. *J. Am. Chem. Soc.* **2007**, *129* (43), 13144–13152.
(10) Han, A.; Creus, M.; Schuermann, G.; Linder, V.; Ward, T.; de Rooij, N.; Staufer, U. *Anal. Chem.* **2008**, *80* (12), 4651–4658.
(11) Fologea, D.; Ledden, B.; McNabb, D. S.; Li, J. *Appl. Phys. Lett.* **2007**, *91*, No. 053901.
(12) Talaga, D. S.; Li, J. *J. Am. Chem. Soc.* **2009**, *131* (26), 9287–9297.
(13) Dekker, C. *Nat. Nanotechnol.* **2007**, *2* (4), 209.
(14) Wanunu, M.; Meller, A. *Nano Lett.* **2007**, *7* (6), 1580–1585.
(15) Vlassiouk, I.; Kozel, T. R.; Siwy, Z. S. *J. Am. Chem. Soc.* **2009**, *131* (23), 8211–8220.
(16) He, Y.; Gillespie, D.; Boda, D.; Vlassiouk, I.; Eisenberg, R. S.; Siwy, Z. S. *J. Am. Chem. Soc.* **2009**, *131* (14), 5194–5202.
(17) Squires, T. M.; Quake, S. R. *Rev. Mod. Phys.* **2005**, *77* (3), 977–1026.
(18) van der Heyden, F. H. J.; Stein, D.; Dekker, C. *Phys. Rev. Lett.* **2005**, *95* (11), 116104.
(19) King, T. L.; Gatimu, E. N.; Bohn, P. W. *Biomicrofluidics* **2009**, *3* (1), 012004–11.
(20) Miller, S.; Young, V.; Martin, C. *J. Am. Chem. Soc.* **2001**, *123* (49), 12335–12342.
(21) Vlassiouk, I.; Smirnov, S.; Siwy, Z. *Nano Lett.* **2008**, *8* (7), 1978.
(22) Yusko, E. C.; An, R.; Mayer, M. *ACS Nano* **2009**, *4* (1), 477–487.
(23) Wong, C. T. A.; Muthukumar, M. *J. Chem. Phys.* **2007**, *126* (16), 164903–6.
(24) Gu, L. Q.; Cheley, S.; Bayley, H. *Proc. Natl. Acad. Sci.U.S.A.* **2003**, *100* (26), 15498.
(25) Ohshima, H. *J. Colloid Interface Sci.* **1994**, *168* (1), 269–271.
(26) Green, N. M. *Biochem. J.* **1963**, *89*, 609–620.
(27) Tangsuphoom, N.; Coupland, J. N. *J. Food Sci.* **2008**, *73* (6), No. E274−E280.
(28) Obi, I.; Ichikawa, Y.; Kakutani, T.; Senda, M. *Plant Cell Physiol.* **1989**, *30* (1), 129–135.
(29) Gustafsson, J.; Mikkola, P.; Jokinen, M.; Rosenholm, J. B. *Colloids Surf., A* **2000**, *175* (3), 349–359.
(30) Smolyanitsky, A.; Saraniti, M. *J. Comput. Electron.* **2009**, *8* (2), 90–97.
(31) Storm, A. J.; Chen, J. H.; Ling, X. S.; Zandbergen, H. W.; Dekker, C. *Nat. Mater.* **2003**, *2* (8), 537–540.

DOI: 10.1021/nl100861c | *Nano Lett.* **2010,** *10,* 2162–2167

(32) Kirby, B. J.; Hasselbrink, E. F. *Electrophoresis* **2004**, *25* (2), 187–202.
(33) Hunter, R. *Zeta Potential in Colloid Science*; Academic Press: New York, 1981.
(34) Harame, D. L.; Bousse, L. J.; Shott, J. D.; Meindl, J. D. *IEEE Trans. Electron Devices* **1987**, *34* (8), 1700–1707.
(35) Mikolajick, T.; Kühnhold, R.; Schnupp, R.; Ryssel, H. *Sens. Actuators, B* **1999**, *58* (1−3), 450–455.
(36) Bousse, L. J.; Mostarshed, S. *J. Electroanal. Chem.* **1991**, *302*, 269–274.
(37) Bousse, L. J.; Mostarshed, S.; Hafeman, D. In Combined measurement of surface potential and zeta potential at insulator/electrolyte interfaces; TRANSDUCERS '91; *International Conference on Solid-State Sensors and Actuators: Digest of Technical Papers*; IEEE: Piscataway, NJ, 1991; pp 502−505.
(38) Bousse, L.; Hafeman, D.; Tran, N. *Sens. Actuators, B* **1990**, *1* (1−6), 361–367.
(39) Pedone, D.; Firnkes, M.; Rant, U. *Anal. Chem.* **2009**, *81* (23), 9689–9694.

DOI: 10.1021/nl100861c | *Nano Lett.* **2010,** *10,* 2162--2167